

# Sodium resonance fluorescence lidar for the measurements of mesopause region temperature and wind over Hainan, China (109 °E, 19.5 °N)

Xingjin Wang<sup>(a)</sup>, Xin Fang<sup>(a)</sup>, Xianghui Xue<sup>(a)</sup>

*(a) CAS Key Laboratory of Geospace Environment, School of Earth and Space Sciences, University of Science and Technology of China, Hefei, Anhui, China*

**Abstract:** Recently, we report a sodium resonance fluorescence lidar developed by the University of Science and Technology of China (USTC) in Hainan, China (109 °N, 19.5 °E). The lidar system in addition to high temporal and vertical resolutions at 10s and 61m, also a high system efficiency, high stability and mobility. Compared with the University of Science and Technology of China (USTC) narrowband sodium lidar, the sodium resonance fluorescence lidar was deployed with a number of technical improvements; which include an all-solid-state fiber continuous-wave (CW) laser, frequency locking performed by modulation transfer spectroscopy. Meanwhile, the lidar system was built in a mobile shelter. With the averaged power of ~ 1.5 W output from PDA and the receiving telescope diameter of 1 m, our lidar system has a power aperture product of ~ 1.18 Wm<sup>2</sup> and is better than the CSU and the University of Science and Technology of China at Hefei sodium lidar systems. The sodium resonance fluorescence lidar has been operated regularly during the night since July 2023. The initial lidar data express that the uncertainties of temperature and wind with a 2 km vertical and 30 min temporal resolution are estimated to be ~ 1.2 K and ~ 2.0 m/ s, respectively, at the sodium peak (e.g., 92 km), and 5 K and 10 m/ s, respectively, at both sodium layer edges (e.g., 81 km and 105 km). The sodium resonance fluorescence lidar observations generally accord with satellite observations as well as model simulations at similar latitude.

## 1. Introduction

Since the 1970s, Ground-based instruments (e.g., lidars, radars) and spaceborne instruments have been widely used to measure the temperature and wind in the upper mesosphere and lower thermosphere region (Vincent and Reid., 1983; She et al., 1998; Wu et al., 2008; li et al., 2012; Fang et al., 2012). Compared with the time continuity of satellites and the resolution of medium-frequency radars, narrowband sodium lidar is able to simultaneously measure mesopause region temperature and horizontal wind by utilizing the sodium high-resolution spectrum (Vincent and Reid., 1983; She et al., 1994; Arnold and She., 2003).

The first lidar observations of neutral sodium atoms in the mesopause region were conducted with a broadband laser system (Bowman et al., 1969). On 1979, the first observation of sodium ground-state hyperfine structure in the upper atmosphere was made successfully (Gibson et

al., 1979). The University of Bonn developed the first narrowband sodium temperature lidar using a tunable pulsed dye laser in 1985 (Fricke et al., 1985), which was used to measure the mesopause region temperature for many years in Andenes, Norway (Zahn et al., 1989). The new narrowband sodium lidar was first constructed at Colorado State University (CSU) in collaboration with scientists from the University of Illinois at Urbana-Champaign (UIUC) with a continuous tunable dye laser seed pulsed dye amplifier (PDA), which both measured the temperature and sodium density in the mesopause region (She et al., 1990). The system has been capable of measuring simultaneously temperature and horizontal wind on the 24-hour after upgraded to a three-frequency system since 2002 (She et al., 2004).

In this paper, we report here a sodium resonance fluorescence lidar developed by the University of Science and Technology of China (USTC) in Hainan, China, which is based on an all-solid-state fiber continuous-wave (CW) laser,

following the CSU temperature/wind lidar. Furthermore, this system implemented with a number of improvements over the USTC temperature/wind lidar, enhancing mechanical stability, automation, and efficiency in lidar operation. Specifically, we deployed a more stable 589nm lidar, and implemented with new designs for a more integrated timing control system, as well as a more accurate frequency locking unit with the use of Electro-Optic Modulator (EOM).

## 2. Figures and Tables

The sodium resonance fluorescence lidar includes laser transmitting system, optical receiving system, photoelectric detection system, data processing and control system. The schematic diagram of the sodium resonance fluorescence lidar is shown in Figure 1. And the parameters of the LiDAR systems are shown in Table 1.

Figure 1. Schematic diagram of the lidar

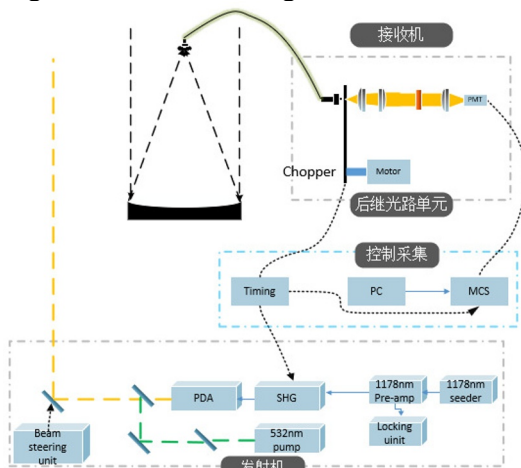


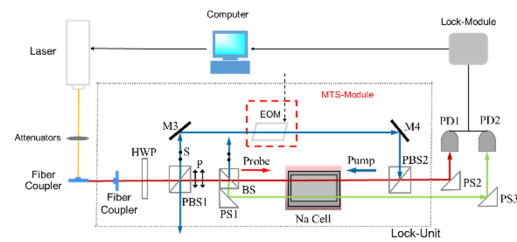
Table 1. Lidar Parameters

	Parameter	Value
Transmitter	Linewidth	120MHz
	Pulse energy	30mJ
	Repetition rate	50Hz
	Pulse width	5ns
	Beam divergence	0.3mrad
Receiver	Telescope aperture	1m
	Field of view	0.88mrad
	Bandwidth	1nm
	Range bin length	61.44m

Our lidar system frequency locking performed by modulation transfer spectroscopy with the use of Electro-Optic Modulator (EOM). The

schematic diagram of the modulation transfer spectroscopy is shown in Figure 2

Figure 2. Schematic diagram of modulation transfer spectroscopy



## 3. Initial Results

The sodium resonance fluorescence lidar has been operated regularly during the night since July 2023. We show some initial lidar data in this section.

The figure 3 show typical nighttime raw photon profiles at three frequencies obtained from a 1 min on January 02, 2024. The blue, red, and yellow curves denote the returning signals at the frequencies of D2a peak, +630 MHz, and -630 MHz, respectively. And the Lidar-observed nighttime hourly mean sodium density is shown in Figure 4.

Figure 3. Raw signals

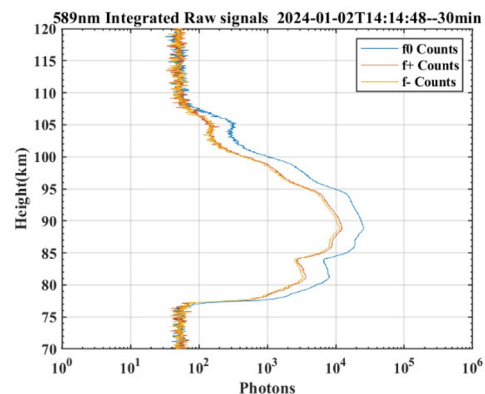
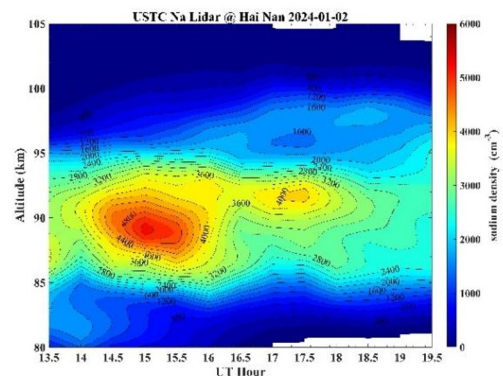


Figure 4. Sodium density



The figure 5 show typical nighttime temperature of sodium layer on January 02, 2024. Comparison of temperature measured by the sodium resonance fluorescence lidar and SABER near Hainan is shown in Figure 6.

Figure 5. Temperature of sodium layer

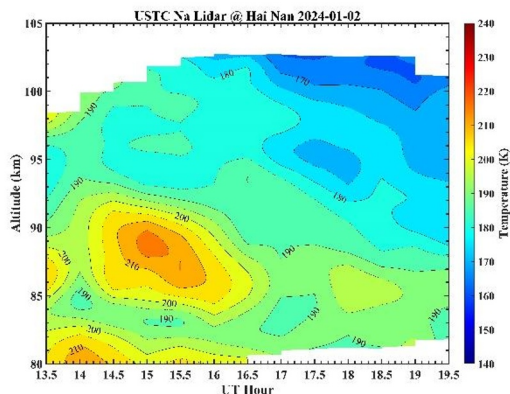
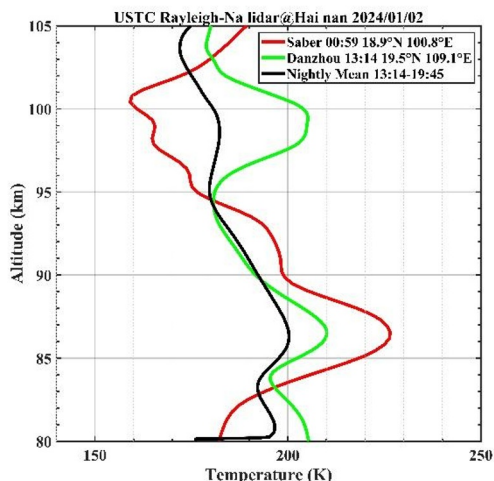
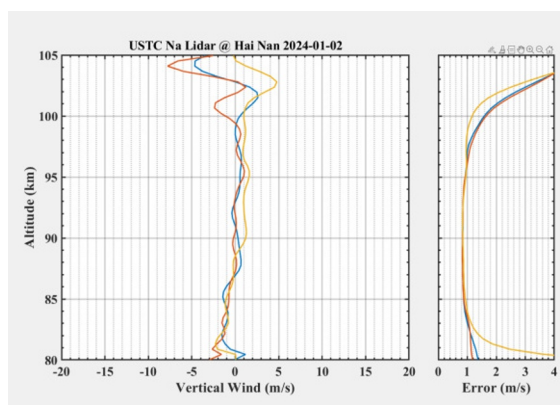


Figure 6. Temperature comparison



The figure 7 show typical nighttime vertical wind of sodium layer on January 02, 2024.

Figure 7. Vertical wind of sodium layer



#### 4. Summary

The sodium resonance fluorescence lidar was developed by the University of Science and Technology of China (USTC) in Hainan, China (109 °N, 19.5 °E) with two key improvements, which include an all-solid-state fiber continuous-wave (CW) laser and frequency locking performed by modulation transfer spectroscopy. The sodium resonance fluorescence lidar has been operated regularly during the night since July 2023. The initial lidar data express that the uncertainties of temperature and wind with a 2 km vertical and 30 min temporal resolution are estimated to be ~ 1.2 K and ~ 3.0 m/ s, respectively, at the sodium peak (e.g., 92 km), and 5 K and 10 m/ s, respectively, at both sodium layer edges (e.g., 81 km and 105 km). The sodium resonance fluorescence lidar observations generally accord with satellite observations at similar latitude.

#### 5. Acknowledgments

This work is supported by Key-Area Research and Development Program of Guangdong Province 2020B0303020001, Ground-based Space Environment Monitoring Network (the Chinese Meridian Project).

#### 6. References

[1] R. A. Vincent, and I. M. Reid, “HF doppler measurements of mesospheric gravity-wave momentum fluxes,” *J. Atmos. Sci.*, 40, 1321–1333 (1983).  
 [2] C. Y. She, S. W. Thiel, and D. A. Krueger, “Observed Episodic Warming at 86 and 100 km Between 1990 and 1997: Effects of Mount Pinatubo Eruption,” *Geophys. Res. Lett.*, 25, 497–500 (1998).  
 [3] Wu. Q. Ortland, D. A. Killeen, T. L. Roble, R. G. Hagan, M.E. Liu, H. L. Solomon, S. C. Xu, J. Skinner, W. R. and R. J. Niciejewski, “Global distribution and interannual variations of mesospheric and lower thermospheric neutral wind diurnal tide: 1. Migrating tide,” *J. Geophys. Res.*, 113, A05308 (2008).  
 [4] Li, T., C. Ban, Xin Fang, J. Li, Z. Wu, J. Xiong, W. Feng and John Maurice Campbell Plane. “Climatology of mesopause region nocturnal temperature, zonal wind, and sodium density observed by sodium lidar over Hefei, China (32°N, 117°E).” *Atmospheric Chemistry and Physics*, 18(16), 11683-11695 (2017).  
 [5] Li, T., Fang, X., Liu, W., Gu, S., & Dou, X. “Narrowband sodium lidar for the measurements of

- mesopause region temperature and wind,” *Applied optics*, 51 22, 5401-11 (2012).
- [6] C. Y. She, and J. R. Yu, “Simultaneous three-frequency Na lidar measurements of radial wind and temperature in the mesopause region,” *Geophys. Res. Lett.*, 21, 1771–1774 (1994).
- [7] K. Arnold, and C. She, “Metal fluorescence lidar (light detection and ranging) and the middle atmosphere,” *Contemp. Phys.*, 44, 35–49 (2003).
- [8] M. R. Bowman, A. J. Gibson, and M. C. W. Sandford, “Atmospheric sodium measured by a tuned laser radar,” *Nature* 221,456– 457 (1969).
- [9] A. J. Gibson, L. Thomas, and S. K. Bhattachacharyya, “Laser observations of the ground-state hyperfine structure of sodium and of temperatures in the upper atmosphere,” *Nature* 281, 131– 132 (1979).
- [10] K. H. Fricke and U. von Zahn, “Mesopause temperature derived from probing the hyperfine structure of the D2 resonance line of sodium by lidar,” *J. Atmos. Terr. Phys.* 47,499– 512 (1985).
- [11] U. von Zahn and W. Meyer, “Mesopause temperatures in polar summer,” *J. Geophys. Res.* 94, 14647– 14651 (1989).
- [12] C. Y. She, H. Latifi, J. R. Yu, R. J. Alvarez II, R. E. Bills, and C. S. Gardner, “Two-frequency lidar technique for mesospheric Na temperature measurements,” *Geophys. Res. Lett.* 17, 929– 932 (1990).
- [13] C. Y. She, T. Li, R. L. Collins, T. Yuan, B. P. Williams, T. D. Kawahara, J. D. Vance, P. Acott, and D. A. Krueger, “Tidal perturbations and variability in mesopause region over Fort Collins, CO (41 N, 105 W): continuous multi-day temperature and wind lidar observations,” *Geophys. Res. Lett.* 31 (2004).